ANALYSIS OF THE IN-PLANE SHEAR BEHAVIOUR OF BIAXIAL NON-CRIMP-FABRIC AT MESOSCOPIC SCALE

R. ZHENG[1*], B. Schäfer[2], N Naouar[1], J. Colmars[1], A. Plazer[1], P. Boisse[1]
[1] Univ Lyon, INSA-Lyon, CNRS UMR5259, LaMCoS, F-69621, France,
[2] Karlsruhe Institute of Technology (KIT), Institute of Vehicle System Technology (FAST), Karlsruhe, Germany
[*] Ruochen ZHENG (ruochen.zheng@insa-lyon.fr)

Keywords: In-plane shear, NCF, Bias-extension test, Finite element model, Meso scale

ABSTRACT

Understanding the mechanical properties of carbon fibre reinforcements is necessary for the simulation of forming processes, where the in-plane shear is one of the basic deformation mechanisms. In this paper, the shear deformation mechanics of warp-knitted 0°/90° carbon fibre biaxial non-crimp fabric (NCF) were experimentally investigated based on a bias-extension test. For NCF, the interplay sliding and the development of gap between fibre yarns caused by stretched stitches are two mechanisms which differ from those observed in woven fabrics and are challenging to directly detect through macroscopic studies that treat the entire structure as a continuous medium. A mesoscopic-scale representative unit cell model with accurate geometrical parameters was utilized to conduct an in-plane shear simulation. The local deformation of fibre yarns and stitches including the change of width and the development of gap can be visualized and the normalized shear force were compared between the experimental results and simulation results.

1 INTRODUCTION

Non-crimp fabrics (NCF) are unique among textile composite reinforcements because its fibre yarns in both directions are straight without any waviness and each of them is bound with a stitching loop along a specific direction that can be adapted to a desired formability. This specific geometry provides NCF with advantageous combinations of properties [1], making them increasingly used nowadays in various areas such as aeronautic and automotive [2]. In order to improve the accuracy of the prediction of the fabric draping in simulation and the quality of final components, a deeper understanding of the in-plane shear deformation is necessary, as it plays a crucial role in NCF's forming behaviour [3].

The in-plane shear behaviour of composite reinforcements has been extensively investigated through two main experimental tests, namely the Picture Frame test and the Bias-extension test [4]. Studies have shown that the initial tension of fibre yarn in the Picture Frame test affects the response in shearing, resulting in a larger shear force [5]. On the other hand, the Bias-extension test is advantageous due to the absence of spurious tensions in the yarn and its relative simplicity and moderate size [6]. However, for biaxial non-crimp fabrics, slippage between the two plies of carbon fibre yarn occurs and should not be neglected [7]. Moreover, tensioned stitches alter the spacing between adjacent fibre yarns, which can impact the fulfil of resin in liquid moulding processes and cause a "rich resin area" if the gap is too large. To predict the slippage between fibre plies and the development of gap, a macroscopic model may encounter difficulties because the entire fabric is considered as a solid medium. A numerical result of the in-plane transverse strain from a macroscopic model can be used to analyse [8, 9] but is not able to detect the gap directly. Thus, the mesoscopic models with fiber yarns and stitches constructed individually were proposed and developed by many researchers [3, 10] (Figure 1).

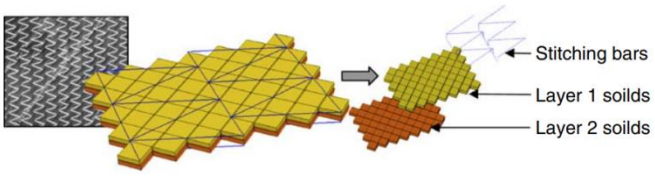

Figure 1. A mesoscopic model of tricot-stitch biaxial non-crimp fabric [10]

To accurately capture the changes in gap, it is necessary to develop a detailed model in the mesoscopic scale. X-ray tomography is a useful tool to obtain the 3D internal geometry [11], while a tracer fibre technique has been used to determine the stitch geometry for a detailed geometric model of glass fibre non-crimp fabric [12]. Additionally, software programs such as TexGen or WiseTex can also be used to create these models [13, 14].

In this study, a model is created using the geometrical parameters obtained from X-ray tomography measurements, and a hyperelastic constitutive law is used to describe the mechanical properties of carbon fibre yarn. A bias-extension test simulation is then performed in software Abaqus and compared to experimental results, with particular attention given to the yarn's compression, slippage, development of gap, and shear force. By accurately modelling these factors, a better understanding of the in-plane shear behaviour of non-crimp fabrics can be achieved.

2 MATERIAL AND NUMERICAL MODEL

Material The material that was used for the experiments in this study is a warp-knitted 0°/90° carbon fibre biaxial NCF with polyester tricot stitches produced by Zoltek. The two layers are bound together during the production process with loop formation in the warp direction. The photographs of bi-axial NCF on both sides are shown in Figure 2. The material parameters are shown in Table 1 from the technical documents of Zoltek.

(a)  (b) 

Figure 2. 0°/90° tricot-stitch biaxial non-crimp fabric architecture (a) warp fibre yarn view with a tricot stitch pattern (b) weft fibre yarn view with a chain stitch pattern

Material	Fiber Orientation	Nominal weights g/m2
ZOLTEK PX35 50K	0°	300(8.85)
ZOLTEK PX35 50K	90°	300(8.85)
Polyester Stitch		8(.235)

Table 1: Material parameters of 0°/90° tricot-stitch biaxial non-crimp fabric

Geometrical model The geometric modelling of biaxial non-crimp fabric (NCF) at a mesoscopic scale involves separate modelling of stitches and fibre yarns. The cross-section shape of fibre yarn was assumed to be circular, flat, elliptic or biconvex in several researches [16, 17]. In this study, the fibre yarns are initially constructed as oval shapes in cross-sections and are assumed to be straight along the fibre orientation, neglecting small distortions created by the tensioned stitch. The position of nodes is calculated using an elliptic cylinder 3D equation with a Matlab script, considering the mesh size, and eight nodes form a solid element.

The nodes on a single loop of stitch are calculated using the equilibrium equation of the elliptical fibre yarn and are shown in Figure 3a. The one loop of stitch wraps around the fibre yarn from A to B, pierces the two fibrous plies from B to C, wraps around another direction's fibre yarn from C to D, and then wraps around the previous loop from D to E. These steps are repeated from E to H, and two nodes form a beam element for using in the simulation. After assembling the fibre yarns and stitches, a simulation of the shrinkage of the stitch is conducted aiming to tighten the initial loose structure and

establish effective interaction between the yarn systems [18]. The mesoscopic geometrical model of biaxial NCF is presented in Figure 3b and 3c.

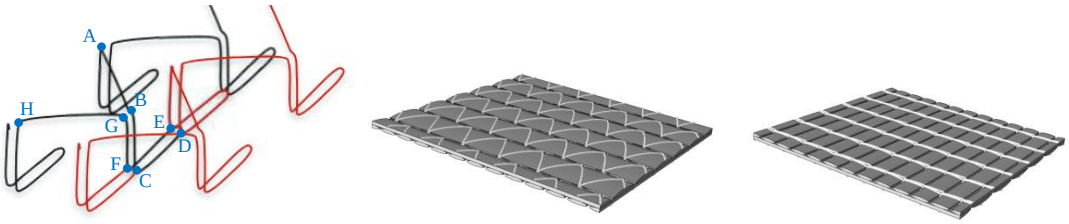

(a) (b) (c)

Figure 3. Numerical model of biaxial NCF (a) schema of tricot stitching pattern [15] (b) warp yarn view of geometrical model (c) weft yarn view off geometrical model

Mechanical behaviour The polyester stitch is modelled as a linear elastic material, while a hyperelastic constitutive law developed by Charmetant is employed for the carbon fibre yarn [19]. The stresses are derived from a strain energy potential that describes the mechanical behaviour of a single carbon fibre yarn. The fibre yarn takes into account four deformation modes, including elongation along the fibre direction, compaction of the cross section, transverse shear (distortion of the cross section), and longitudinal shear along the fibre direction based on the assumption that the fibre yarn is transverse isotropy.

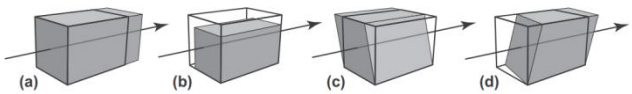

Fig. 4. Four deformation modes of fiber yarn (a) elongation (b) compaction of cross section (c) transverse shear (d) longitudinal shear

Thus, the deformation gradient tensor, $\underline{F}$, which allows the transformation of fiber yarn from its initial position $\underline{X}$ to its deformed position $\underline{x}$, can be split into four matrixes associated with these four deformation modes.

$$\left[\underline{F}\right] = \left[\underline{F_{\text{elong}}}\right] \vdots \left[\underline{F_{\text{comp}}}\right] \vdots \left[\underline{F_{\text{dist}}}\right] \vdots \left[\underline{F_{\text{sh}}}\right] \tag{1}$$

The hyperelastic equation defines the material's elastic strain energy potential based on the strain state. Four physically based invariants I_{elong}, I_{comp}, I_{dist}, I_{sh} are defined as a function of the classical invariants I_1 to I_5 of the right Cauchy Green strain tensor $\underline{C}$ and then used to describe these different deformation modes.

These physically based invariants are introduced in [22] and are expressed as:

$$I_{\text{elong}} = \frac{1}{2}\ln I_4,\ I_{\text{comp}} = \frac{1}{4}\ln\left(\frac{I_3}{I_4}\right),\ I_{\text{dist}} = \frac{1}{2}\ln\left(\frac{I_1 I_4 - I_5}{2\sqrt{I_3 I_4}} + \sqrt{\left(\frac{I_1 I_4 - I_5}{2\sqrt{I_3 I_4}}\right)^2 - 1}\right),\ I_{\text{sh}} = \sqrt{\frac{I_5}{{I_4}^2} - 1} \tag{2}$$

Where these classical invariants are expressed by the right Cauchy Green strain tensor $\underline{C}$ and a structural tensor $\underline{M}$ defined by a unit vector of fibre direction $\underline{M}$ as:

$$I_1 = \text{trace}(\underline{C}),\ I_2 = \frac{1}{2}\left(\text{trace}\left(\underline{C}\right)^2 - \text{trace}(\underline{C^2})\right),\ I_3 = \det\left(\underline{C}\right),\ I_4 = \underline{C} : \underline{M},\ I_5 = \underline{C^2} : \underline{M} \tag{3}$$

Then the deformation energy is assumed to be the sum of the energies of these four deformation modes:

$$w(F) = w_{\text{elong}}(I_{\text{elong}}) + w_{\text{comp}}(I_{comp}) + w_{\text{dist}}(I_{\text{dist}}) + w_{\text{sh}}(I_{\text{sh}}) \tag{4}$$

The second Piola–Kirchhoff stress tensor is defined as:

$$\underline{\underline{S}} = 2\frac{\partial w}{\partial \underline{\underline{C}}} = 2\left(\frac{\partial w_{\text{elong}}}{\partial I_{\text{elong}}}\frac{\partial I_{\text{elong}}}{\partial \underline{\underline{C}}} + \frac{\partial w_{\text{comp}}}{\partial I_{\text{comp}}}\frac{\partial I_{\text{comp}}}{\partial \underline{\underline{C}}} + \frac{\partial w_{\text{dis}}}{\partial I_{\text{dis}}}\frac{\partial I_{dis}}{\partial \underline{\underline{C}}} + \frac{\partial w_{\text{sh}}}{\partial I_{\text{sh}}}\frac{\partial I_{\text{sh}}}{\partial \underline{\underline{C}}}\right) \tag{5}$$

Experimental traction tests and compaction tests on single carbon fibre yarn were carried out in several researches [22] [25] and inverse approaches were used to identify the parameters. Since the studied Bi-NCF is also made of carbon fibres, the same material parameters are used.

3 BIAS EXTENSION TEST

In this study, the bias-extension test was conducted. A rectangular specimen measuring 50mm*150mm in width (W) and length (L) was cut with yarns initially oriented at ±45° to the direction of the applied tension. The bottom side of the specimen was held in a fixed position, while the top side was subjected to a stretching force. The stretching was applied at a speed of 25mm/min.

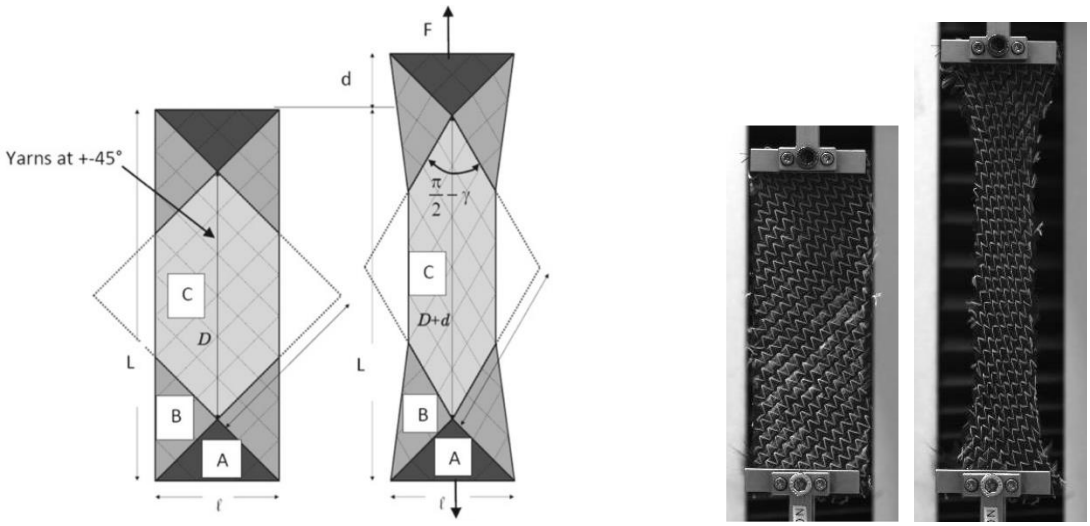

(a) (b)

Figure 5. Bias-extension test (a) Schema [6] (b) Experimental test

The standard bias-extension test assumes that the fibre yarns are inextensible, and there is no slip between the warp and weft yarns [6]. After stretching the fabric from L to L+d (where d is the tensile machine displacement), three zone can be observed on the deformed shape as shown in Figure 5a: an undeformed zone A due to the clamp of one end of fibre yarn, a shear zone C which has free ends and a half shear zone B. The shear angle of the middle shear zone C can be calculated by the kinematic relation between the shear angle γ and the length of specimen L if it is a pure shear zone and no slip happens:

$$\gamma = \frac{\pi}{2} - 2\cos^{-1}\frac{D+d}{\sqrt{2}D}, \tag{6}$$

Where

$$D = L - W \tag{7}$$

However, in the case of NCF, there is more slip between the weft and warp yarn, leading to a lower true shear angle. Previous studies have shown that the true shear angle is below 5° when the shear angle is less than 30°, and it increases beyond this point [3]. As shown in Figure 5b, the presence of numerous individual yarns along the edges of zone B provides evidence of interply sliding. Two cameras were

used to focus on the intermediate shear zone for a zoomed-in view to measure the change in angle between the two fibre yarn layers, as well as the development of gap between adjacent fibre yarn and the width of fibre yarn. Figure 6 shows the zoomed-in view of warp yarn. Five fibre yarns were noted by white lines so that it could be followed during the shear deformation. The gaps between the fiber yarns vary depending on their initial size, so to accurately follow the changes in gap size, the measured values are normalized by dividing them by the initial values before making any comparisons.

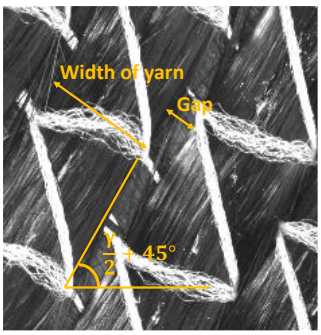

Figure 6. A zoomed in view of Bias-extension test

The normalized shear force can be obtained by [4]:

$$F_{\mathrm{sh}}(\gamma) = \frac{1}{(2H-3W)\cos\gamma}\left(\left(\frac{H}{W}-1\right)\cdot F\cdot\left(\cos\frac{\gamma}{2}-\sin\frac{\gamma}{2}\right)-W\cdot F_{\mathrm{sh}}\left(\frac{\gamma}{2}\right)\cos\frac{\gamma}{2}\right) \tag{8}$$

At a certain shear angle γ, the shear force is computed by the machine force F, which is a known value and the shear force at $\frac{\gamma}{2}$, which is an unknown value. However, the shear force at $\frac{\gamma}{2}$ can be computed by the shear force at $\frac{\gamma}{4}$. Thus, if we consider that the shear force is 0 when the shear angle is very small (like 10^{-7}), an iterative algorithm can then be used for this computation through a MATLAB script and the result is shown in Fig. 8 to compare with the numerical results.

4 SIMULATION AND DISCUSSION

A representative unit-cell model with dimensions of 10*10mm was initially employed to simulate the in-plane shear deformation of $0^{\circ}/90^{\circ}$biaxial NCF based on the assumption that it is a periodic medium, with a boundary condition that proposed by Badel [21]. The model consisted of half fiber yarns along the boundary and a complete yarn and stitch loop at the center. The fiber yarns were modelled by solid elements, while the stitches were modelled by finite beam elements. The nodes on one corner were fixed while the opposite corner was stretched at a $\pm 45°$ to the two fiber directions.

Figure 7 displays a comparison of the initial and deformed configurations of the unit cell under various shear angles, alongside the zoomed-in view of the bias-extension test. In contrast to a ±45° tricot stitch biaxial NCF, which exhibits positive and negative shear due to the structure, the $0^{\circ}/90^{\circ}$biaxial NCF demonstrates symmetric behavior during shearing. One segment of the stitch is consistently stretched, while the other remains loose. The fiber yarn is continuously compressed by the tensioned stitch. The slippage between yarn and stitch can be seen and the loose stitch becomes nearly perpendicular to the fiber orientation at the end. Both the simulation and experimental findings corroborate that the gap between adjacent fiber yarns gradually widens due to yarn compression until reaching approximately $25-30^{\circ}$. Subsequently, the gap begins to decrease until it reaches zero when the fiber yarns contact each other.

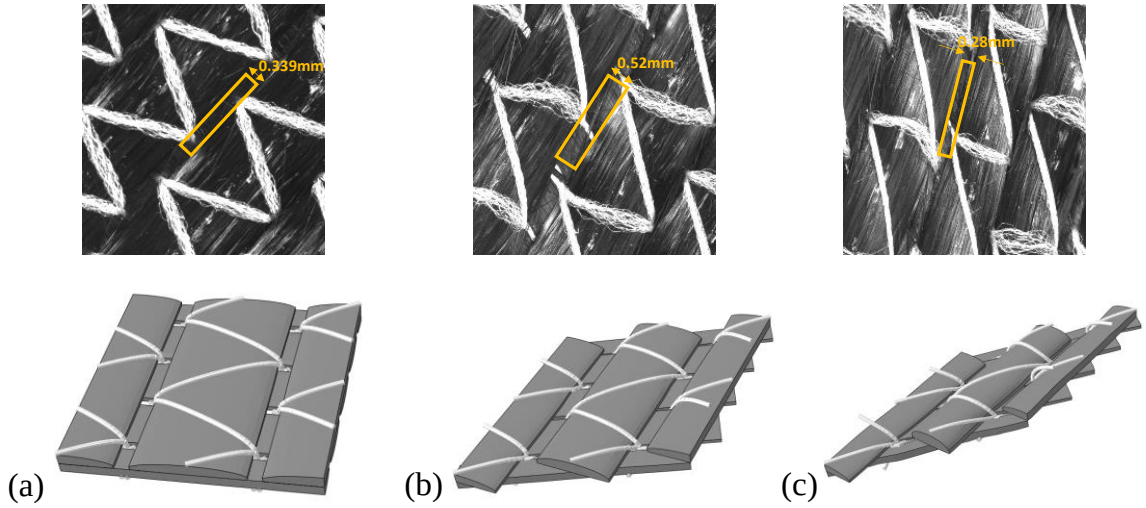

Figure 7. Bias-extension test zoom-in view and unit cell in-plane shear simulation under different shear angle (a) initial configuration (b) 26° (c) 52°

The simulation results of normalized shear force and shear angle are shown in Fig. 8, showing a good agreement with the experimental results.

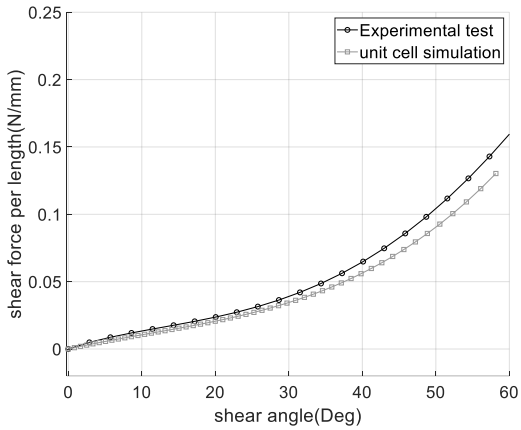

Figure 8. Shear force normalized vs. shear angle

5 CONCLUSIONS

In this study, a bias-extension test was conducted to investigate the in-plane shear behaviour of warp-knitted 0°/90° carbon fibre biaxial non-crimp fabric (NCF) with polyester tricot stitches. To accurately capture the intricate details, a mesoscopic finite element model was developed, incorporating precise geometric parameters. The zoom-in view of the bias-extension test and the representative unit cell modelling demonstrate the advantages of detecting local deformations and defects compared to macroscopic simulations.

This modelling approach enables direct visualization of yarn width, gap development, and interlayer sliding. The excellent agreement between the shear forces obtained from the bias-extension test and the unit cell modelling validates the potential of this model for virtual material testing, significantly reducing the reliance on extensive experimental tests. Moreover, the adjustability of stitch geometry and yarn cross-section facilitates the analysis of various stitching patterns, offering the possibility to develop customized NCFs with optimized deformation behaviour for specific applications.

ACKNOWLEDGEMENTS

This work is funded by the French National Research Agency (ANR) and the Deutsche

Forschungsgemeinschaft (DFG, German Research Foundation) in the collaborative project AMECOMP "Composite forming simulation for non-crimp fabrics based on generalized continuum approaches".

REFERENCES

[1] S. Bel, P.Boisse, F. Dumont, Analyses of the Deformation Mechanisms of Non-Crimp Fabric Composite Reinforcements during Preforming, *Applied Composite Materials*, **19**, 2012, pp. 513-528 (doi: 10.1007/s10443-011-9207-x).

[2] P. Middendorf, C. Metzner, Aerospace applications of non-crimp fabric composites, in: Stepan V. Lomov (Eds.), Non-Crimp Fabric Composites, Woodhead Publishing, 2011, pp. 441-449 (doi: 10.1533/9780857092533.4.441).

[3] Long Li, Yan Zhao, Ha-gia-nam Vuong, Yuan Chen, Jin Yang, Yuexin Duan, In-plane shear investigation of biaxial carbon non-crimp fabrics with experimental tests and finite element modeling, *Materials & Design*, **63**, 2014, pp. 757-765 (doi: 10.1016/j.matdes.2014.07.007).

[4] J. Cao, R. Akkerman, P. Boisse, J. Chen, H.S. Cheng, E.F. de Graaf, J.L. Gorczyca, P. Harrison, G. Hivet, J. Launay, W. Lee, L. Liu, S.V. Lomov, A. Long, E. de Luycker, F. Morestin, J. Padvoiskis, X.Q. Peng, J. Sherwood, Tz. Stoilova, X.M. Tao, I. Verpoest, A. Willems, J. Wiggers, T.X. Yu, B. Zhu, Characterization of mechanical behavior of woven fabrics: Experimental methods and benchmark results, *Composites Part A: Applied Science and Manufacturing*, **39**, 2008, pp. 1037-1053 (doi: 10.1016/j.compositesa.2008.02.016).

[5] Launay, Jean & Hivet, G. & Duong, Ahn & Boisse, Philippe, Experimental analysis of in plane shear behaviour of woven composite reinforcements. Influence of tensions, *Composites Science and Technology*, **68**, 2008, pp. 506-515 (doi: 10.1016/j.compscitech.2007.06.021).

[6] P. Boisse, N. Hamila, E. Guzman-Maldonado, A. Madeo and G. Hivet, F. dell'Isola, The bias-extension test for the analysis of in-plane shear properties of textile composite reinforcements and prepregs: a review, *International Journal of Material Forming*, **10**, 2017, pp. 473-492 (doi: 10.1007/s12289-016-1294-7).

[7] R.H.W. ten Thije and Remko Akkerman, Finite element simulation of draping with non-crimp fabrics, *15th International Conference on Composite Materials, ICCM-15, 2005, Durban, South Africa, June 27- July 1, 2005,* Conference number: 15.

[8] J. Schirmaier, D. Dörr, F. Henning, and L. Kärger, A macroscopic approach to simulate the forming behaviour of stitched unidirectional non-crimp fabrics (UD-NCF), *Composites: Part A*, **102**, 2017, pp. 322-335 (doi: 10.1016/j.compositesa.2017.08.009).

[9] S. Galkin, E. Kunze, L. Kärger, R. Böhm, M. Gude, Experimental and Numerical Determination of the Local Fiber Volume Content of Unidirectional Non-Crimp Fabrics with Forming Effects, *Journal of Composites Science*, 2019, 3, 19. (doi: 10.3390/jcs3010019).

[10] G. Creech, A. K. Pickett, Meso-modelling of Non-Crimp Fabric composites for coupled drape and failure analysis, *Journal of Materials Science*, **41**, 2006, pp. 6725-6736 (doi: 10.1007/s10853-006-0213-6).

[11] N. Naouar, D. Vasiukov, C. H. Park, S. V. Lomov, and P. Boisse, Meso-FE modelling of textile composites and X-ray tomography, *Journal of Materials Science*, **55**, 2020, pp. 16969-16989 (doi: 10.1007/s10853-020-05225-x).

[12] W. Wu, W. Li, Parametric modeling based on the real geometry of glass fiber unidirectional non-crimp fabric, *Textile Research Journal*, **89**, 2019, (doi: 10.1177/0040517518824846).

[13] Lomov, Stepan and Verpoest, I. and Cichosz, Joerg and Hahn, Christoph and Ivanov, Dmitry, Meso-level textile composites simulations: Open data exchange and scripting, *Journal of Composite Materials*, **48**, 2014, pp. 621-637 (doi: 10.1177/0021998313476327).

[14] L.P. Brown and A.C. Long, Modeling the geometry of textile reinforcements for composites: TexGen, in: Philippe Boisse (Eds.), Composite Reinforcements for Optimum Performance (Second Edition), Woodhead Publishing, 2021, pp. 237-265 (doi: 10.1016/B978-0-12-819005-0.00008-3).

[15] Q. Steer, J. Colmars, P. Boisse, Modeling of tricot stitch non crimp fabric in forming simulations, *AIP Conference Proceedings*, 2 July 2019; 2113 (1): 020004, (doi: 10.1063/1.5112509).

[16] S.V. Lomov, G. Huysmans, Y. Luo, R.S. Parnas, A. Prodromou, I. Verpoest, F.R. Phelan, Textile composites: modelling strategies, *Composites: Part A*, **32**, 2001, (doi: 10.1016/S1359-835X(01)00038-0).

[17] J. Whitcomb, X. Tang, Effective Moduli of Woven Composites, *J Compos Mater*, **35**, 2001, (doi: 10.1177/002199801772661380).

[18] M. Q. Pham, E. Wendt, E. Häntzsche, T. Gereke, C. Cherif, Numerical modeling of the mechanical behavior of textile structures on the meso-scale for forming process simulations of composite 3D preforms, *Engineering Reports*, **4**, 2022, (doi: 10.1002/eng2.12348).

[19] A. Charmetant, E. Vidal-Sallé, P. Boisse, Hyperelastic modelling for mesoscopic analyses of composite reinforcements, *Composites Science and Technology*, **71**, 2011, (doi: 10.1016/j.compscitech.2011.07.004).

[20] A. Iwata, T. Inoue, N. Naouar, P. Boisse, S. V. Lomov, Coupled meso-macro simulation of woven fabric local deformation during draping, *Composite Part A*, **118**, 2019, (doi: 10.1016/j.compositesa.2019.01.004).

[21] P. Badel, E. Vidal-Sallé, P. Boisse, Computational determination of in-plane shear mechanical behaviour of textile composite reinforcements, *Computational Materials Science*, **40**, 2007, (doi: 10.1016/j.commatsci.2007.01.022).